

Spatial Patterns and Characteristics of Flood Seasonality in Europe

Julia Hall¹ and Günter Blöschl¹

¹Institute of Hydraulic Engineering and Water Resources Management, Technische Universität Wien, Vienna, Austria

5 *Correspondence to:* Julia Hall (hall@hydro.tuwien.ac.at)

Abstract.

In Europe, floods are typically analysed within national boundaries and it is therefore not well understood how the characteristics of local floods fit into a continental perspective. To gain a better understanding at continental-scale, this study
10 analyses seasonal flood characteristics across Europe for the period 1960-2010.

From a European flood database, the timing within the year of annual maximum discharges or water levels of 4105 stations is analysed. A cluster analysis is performed to identify large-scale regions with distinct flood seasons on the basis of. ~~The clusters are determined using~~ the monthly relative frequencies of the annual maxima. The clusters ~~and~~ are analysed to determine the temporal flood characteristics within each region and the European-wide patterns of bimodal and unimodal
15 flood seasonality distributions.

Below 60° latitude, the mean timing of floods at individual stations transitions from winter floods in the West to spring floods in the East. Summer floods occurring in mountainous areas interrupt this west to east transition. Above 60° latitude, spring floods are dominant, except for coastal areas in which autumn and winter floods tend to occur ~~are observed~~. The temporal concentration of flood occurrences around a specific time of the year is highest in north-eastern Europe, with most of the
20 floods being concentrated within 1-2 months. The cluster analysis results in six spatially well-defined regions with distinct flood seasonality characteristics. The regions with winter floods in western, central, and southern Europe are assigned to Cluster 1 (~36% of the stations) and Cluster 4 (~10%) with the mean flood timing in late January and early December respectively. In eastern Europe (Cluster 3, ~24%) the average flood occurrence is at the end of March. The floods in northern (Cluster 5, ~8%) and north-eastern-Europe (Cluster 6, ~5%) occur in mid-May and mid-April respectively. About 15% of the
25 stations (Cluster 2) are located in Mountainous ~~mountainous~~ areas with a mean flood timing around the end of June. Most of the stations (~73%) with more than 30 years of data exhibit a unimodal flood seasonality distribution (one or more consecutive months with high flood occurrence). Few stations (~3%), mainly located on the foothills of mountainous areas, have a clear bimodal ~~temporal~~ seasonality distribution. This study suggests that, as a result of the European wide pattern of flood timing, ~~obtained~~ the geographical location of a station in Europe can give an indication of its seasonal ~~temporal~~ flood
30 characteristics and that geographical location seems to be more relevant than catchment area or outlet elevation in shaping flood seasonality.

1 Introduction

Understanding the spatial and temporal characteristics of floods across Europe is important for improving our understanding of the flood generation mechanisms and hence for enabling better flood estimation and forecasts at European scale. River floods in Europe are caused by several processes. The most common naturally occurring river floods are driven by rainfall (including rain on snow) and snowmelt (sometimes combined with ice jams) and are modulated by soil moisture (Hall et al., 2014). Hence, depending on the time of the year (i.e. season) in which a flood peak occurs one can infer the hydrological processes that likely generated the flood. For example, flood peaks occurring in late winter or early spring, together with rising temperatures, are likely to be snowmelt induced. A better knowledge of the flood seasonality can therefore assist in the identification of homogeneous regions with a dominant flood season, which is important for example for regional flood frequency analysis, the analysis of mixed flood frequency distributions, and in the identification and attribution observed changes in flood discharges. Additionally, such homogeneous regions can serve as a benchmark for the assessment of European-wide hydrological model output.

Previous research on flood seasonality in Europe has been limited by two main constraints. First, the focus of most studies has been on national scale or on smaller regions, which limited the analysis to a relatively small and local set of flood-generating processes. For example, Beurton and Thielen (2009) determined three homogeneous flood regions in Germany when analysing the annual maximum floods (AMF) of 481 gauging stations. Similarly, Cunderlik et al. (2004) found three main flood seasonality types in Great Britain examining 268 sites. A few studies analysed flood seasonality at larger scales, for example Mediero et al. (2015) using 102 streamflow records within Europe, but with limited spatial coverage, and Blöschl et al. (2017) focusing on changes in flood seasonality. Second, most of the previous studies on flood seasonality focused on the mean date of the AMF occurrence and/or the temporal concentration of the floods around their mean date (e.g. Parajka et al. (2009) or Jeneiová et al. (2016) for both Austria and Slovakia), while the detailed characteristics of monthly flood seasonality distributions has rarely been studied in Europe. However, if unimodal, bimodal or skewed seasonality distributions exist, the mean date of the AMF can be misleading and can mask important insights into the flood generating mechanisms (Ye et al., 2017). It is therefore important to report not only the mean date to characterise flood seasonality, but to describe also in detail the temporal flood seasonality characteristics.

This paper examines the spatial and temporal patterns of flood seasonality at continental scale, using an extensive database that covers all climatic regions in Europe. The focus of this paper is on the identification of regions with similar seasonal flood characteristics and on the description of the full temporal distribution of the flood events within the year.

First, the study area and the European discharge data set used in this study are presented, followed by the analysis methods. In the results section, the spatial characteristics of the mean flood seasonality are presented together with an analysis of the seasonal flood characteristics across Europe. Spatial patterns and clusters are identified based on the monthly distribution of AMFs. The clusters are then examined in detail, focusing on their monthly flood seasonality characteristics and their spatial distribution. The paper concludes with a discussion of the results and the conclusion.

2 Study Area and Data

The hydrological data analysed here is based on the dataset presented by Hall et al. (2015) subsequent updates. The database used as a starting point in this study includes data from 5565 hydrometric stations from 38 data sources (see Supplement for details) located within 6.5° W - 60° E and 29.25° N - 69.25° N (Fig. 1). Floods events are identified following the common definition as the highest (peak) event in a year (e.g. (Garner et al., 2015; Hall et al., 2014), which does not necessary imply that the river overtops its banks and flows onto the floodplain. Following this definition, the dataset consists of the dates of annual maximum discharge or annual maximum water level (daily mean or instantaneous values). The maximum of each year is based on the calendar year (January to December) with a few exceptions, which are based on the respective countries' hydrological year (which can start in September, October, or November). Only the annual maxima are analysed here, as the long-term mean of the flood timing is more meaningful if a single flood peak per year is considered and, additionally, due to restrictions in data access and licensing only the maxima data is available for some areas and/or countries.



Figure 1. Map of Study area, showing the topography and the location of the 4105 stations used in this study.

Catchments for which it was evident that the flood timing is strongly affected by known human modifications (e.g. dams or reservoirs) are excluded from the analysis. All catchments with more than 10 years of data within the period 1960-2010 were included in the first part of the analysis. In areas with high station densities, such as Austria, Germany, and Switzerland, only stations with at least 49 years of data in the analysis period were included to balance station density and to improve the visual representation on a European map. This selection resulted in 4105 hydrometric stations (Fig. 1) with station elevation ranging from -5.17 m to 1961 m (Fig. 2a), catchment areas ranging from 10 km² to 100,000 km² (Fig. 2b) and record lengths ranging from 11 years to 51 years (Fig. 3). 115 stations in the database have no catchment area assigned, either due to the existence of karst or missing metadata information. These stations are not shown in subsequent figure that display catchment area, which is indicated by a reduced number of stations in the figure caption.

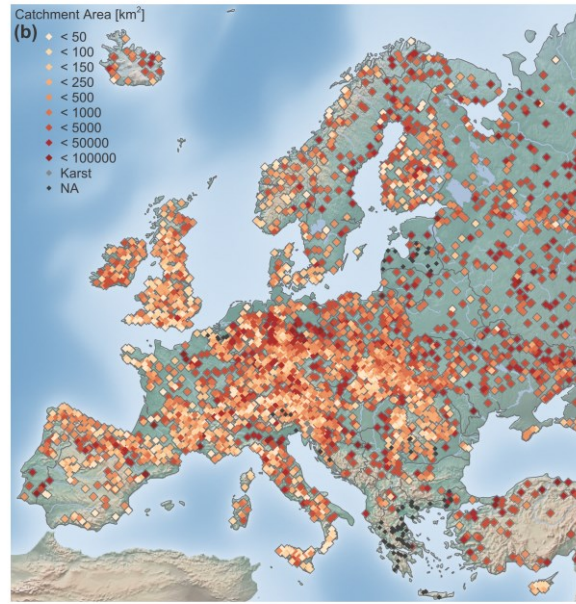
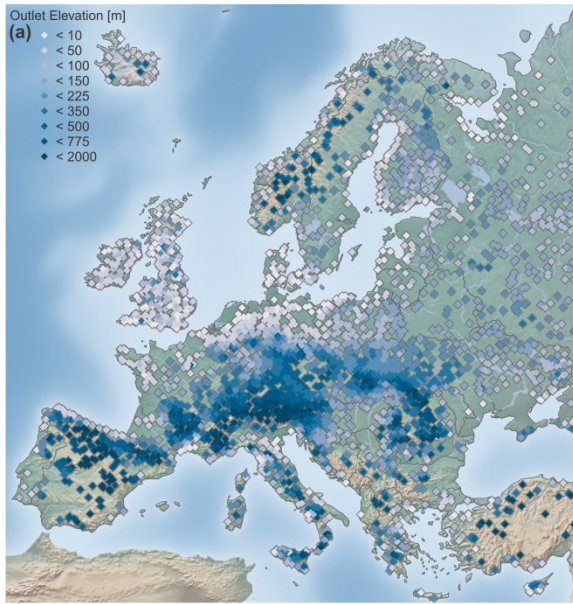


Figure 2. Maps of station elevation at the catchment outlet [m] (a) and catchment area [km²] (b). In both panels, $n=4105$ stations.



Figure 3. Record length in number of years per station for the period 1960-2010, $n = 4105$ stations.

3 Methods

3.1 Flood seasonality

3.1.1 Mean flood seasonality and temporal flood concentration

The mean seasonality of annual maximum floods is determined using circular statistics (Bayliss and Jones, 1993; Mardia, 1972). In order to be able to calculate the mean date of flood occurrence \bar{D} (i.e. day of year (DOY)) for a given station, the date of the flood occurrence D_i (DOY) in year i is converted into an angular value θ_i in radians through

$$\theta_i = D_i \cdot \frac{2\pi}{m_i} \quad 0 \leq \theta_i \leq 2\pi \quad (1)$$

where $D_i = 1$ corresponds to January 1 and $D_i = m_i$ for December 31, and where m_i is the number of days in that year (365 or 366 for leap years). The mean date of occurrence \bar{D} of a flood at a station is then

10

$$\bar{D} = \begin{cases} \left(\tan^{-1} \left(\frac{\bar{y}}{\bar{x}} \right) \right) \cdot \frac{\bar{m}}{2\pi} & \bar{x} > 0, \bar{y} \geq 0 \\ \left(\tan^{-1} \left(\frac{\bar{y}}{\bar{x}} \right) + \pi \right) \cdot \frac{\bar{m}}{2\pi} & \bar{x} \leq 0 \\ \left(\tan^{-1} \left(\frac{\bar{y}}{\bar{x}} \right) + 2\pi \right) \cdot \frac{\bar{m}}{2\pi} & \bar{x} > 0, \bar{y} < 0, \end{cases} \quad (2)$$

with

$$\bar{x} = \frac{1}{n} \sum_{i=1}^n \cos(\theta_i) \quad (3)$$

$$\bar{y} = \frac{1}{n} \sum_{i=1}^n \sin(\theta_i) \quad (4)$$

15 \bar{x} and \bar{y} are the cosine and sine components of the mean date, respectively, \bar{m} is the mean number of days per year (365.25), and n is the total number of flood peaks at that station during the study period.

In order to be able to interpret the mean seasonality, the Concentration Index R of the dates of AMF occurrence around the mean date is calculated. R can be interpreted as a measure of how well the flood seasonality is defined for a given catchment (Fig. 4b).

20

$$R = \sqrt{\bar{x}^2 + \bar{y}^2} \quad 0 \leq R \leq 1 \quad (5)$$

The Concentration Index R ranges from $R = 0$, representing no temporal concentration (i.e., floods are dispersed throughout the year and the seasonality vector of the individual floods cancel out (reflective symmetry)), to $R = 1$, which indicates that all floods occur on the same day of the year.

5 There is a trade-off between good spatial coverage and the minimum record length needed for meaningful flood seasonality analysis. Based on simulated monthly flood frequencies from a uniform distribution, Cunderlik et al. (2004) recommend care when evaluating the results from records shorter than 30 years, because of the large sampling variability that might either artificially increase or mask the strength of the flood seasonality.

10 In the observational dataset analysed here, the mean values of the flood Concentration Index R change little with different record length from 11 to 51 years (± 0.1 of the overall mean R -value of 0.6, not shown). For the analyses of spatial patterns, priority is given to spatial coverage and therefore all 4105 stations (containing time series with a record length of 11-51 years) are used in the analysis of the mean seasonality, temporal flood concentration and the cluster analysis. In the detailed analysis of the monthly flood characteristics only data with at least 30 years of record are used, as the above approximation of the confidence intervals is only valid for records with at least 30 data points (Section 3.3).

3.1.2 Circular uniformity

15 The spatial characteristics of flood seasonality can only be meaningfully interpreted if the data exhibit one or two preferred seasons in which floods occur (unimodal or bimodal flood seasonality). Therefore, stations for which the null hypothesis of circular uniformity (modified Kuiper's test (Mardia and Jupp, 2008)) cannot be rejected ($\alpha=0.1$) are highlighted (i.e. 186 stations) and analysed for their possible connection with spatial location (Fig. 4b), catchment outlet elevation, and catchment area (Fig. 6). Only stations for which the null hypothesis of circular uniformity can be rejected are included in the remaining
20 analyses (3919 stations), since one of the objectives of the paper is the identification of clusters with distinct flood seasonality characteristics.

3.2 Cluster analysis

A cluster analysis is conducted to identify regions with similar flood seasonality across Europe. Depending on the method chosen, different regional clusters can emerge (Everitt et al., 2011). Here, the clusters are estimated using the k-means
25 clustering algorithm. k-means can be considered superior to hierarchical clustering for the analysed dataset, as k-means clustering is less affected by outliers and can be applied to large datasets, preferably for sample sizes > 500 (Everitt et al., 2011). More information on the k-means clustering algorithm by Hartigan and Wong (1979) used in the calculation (the function '*kmeans*' is part of the R package '*stats*') can be found in R-Core-Team (2016).

30 Twelve clustering variables are used, which contain the relative monthly frequency of flood occurrence for the months January to December. For each station, the monthly frequencies of the AMF are calculated. In order to reduce the influence of wide ranges between the variables used in the k-means clustering, a Z-score standardisation of the variables is performed (Vesanto, 2001). Here, the monthly flood frequencies of all stations are standardised to zero mean and a standard deviation of

one. The standardised monthly flood occurrences are the only input to the k-means clustering algorithm. Geographic location is not used as a clustering variable to allow for an independent evaluation of the clusters, based on the time of flood occurrence only. Clusters consisting of stations with close geographical proximity or similar catchment characteristics can be considered more plausible than clusters for which this is not the case.

5 3.2.1 Selection of the number of clusters

One important step in clustering data is the decision on the number of clusters (k), as this number is not known *a priori*. In this study, different numbers of clusters are examined with the aim of obtaining homogenous groups (clusters) of stations that are as similar as possible (regarding the timing of flood occurrence) within their group but are also as dissimilar as possible from the stations not belonging to their group.

- 10 The performance of the k-means clustering algorithm is assessed using the silhouette value $s(i)$ (Rousseeuw, 1987), which is a measure of how similar a station is to its own cluster compared to the other clusters. Silhouette values range from -1 (high similarity with the neighbouring cluster) to 1, with higher $s(i)$ values indicating that the station has a high similarity to its own cluster.

For a number of k clusters ($k > 1$) the silhouette value $s(i)$ can be calculated using Eq. 6,

$$15 \quad s(i) = \frac{b(i) - a(i)}{\max\{a(i), b(i)\}} \quad (6)$$

where $a(i)$ is the average dissimilarity of all variables (here the average Euclidean distance is used) of station i to all other stations in the same cluster (i.e. how distant the station is, on average, from the other stations) and $b(i)$ is the average dissimilarity to all stations in the neighbouring cluster to station i (i.e. the cluster that has the lowest average dissimilarity from all other clusters). The mean silhouette value over a cluster ($\bar{s}(i)_{cluster}$) thus indicates how similar, on average, the stations in a cluster are, and the mean silhouette value $\bar{s}(i)$ over all stations in the dataset indicates how well the clustering algorithm has assigned the stations to their respective cluster. The number of k clusters that has both the highest $\bar{s}(i)$ and highest individual $\bar{s}(i)_{cluster}$ can be considered the best choice (Rousseeuw, 1987).

- 25 As a second criterion for the selection of k clusters, the ‘Elbow method’ based on the total sum of within-cluster sum of squares (TSS_{within}) is used,

$$TSS_{within} = \sum_{j=1}^k \sum_{i=1}^{n_j} (Y_{ij} - \bar{Y}_j)^2, \quad (7)$$

where k is the number of clusters, j is a specific cluster, and i is a individual station in that cluster, so that Y_{ij} is the i^{th} observation in cluster j . \bar{Y}_j is the mean of Y_{ij} over the range of i .

With an increasing numbers of clusters k , the TSS_{within} decreases. The optimal number of k clusters is determined using the magnitude of the reductions in the TSS_{within} between two consecutive clusters. If the reductions do not decrease much beyond a certain number of k clusters, that number is considered a good choice. After accounting for the sensitivity of the initial centroid placements (see below), the final number of clusters is selected based on first the $\bar{s}(i)$ values and second the Elbow method conditional on the TSS_{within} values.

The k-means clustering algorithm is sensitive to the location of the initial k centroids to which the nearest neighbours are assigned (Steinley (2003)). This sensitivity affects both the selection of the ‘optimal number’ of clusters k and the assignment of stations to a certain cluster. To account for this, the k-mean algorithm is repeated with 10,000 random centroids initialisations (seed vectors) and the initialisation with the highest mean silhouette value over all stations $\bar{s}(i)$ is selected. As several initial centroid locations for k clusters can result in the same maximum $\bar{s}(i)$ value, all centroids initialisations that have the same maximum $\bar{s}(i)$ value are retained and further analysed with regard to their TSS_{within} values. From these initialisations, only the sets of initial centroids that have the same optimal number of clusters k based on the $\bar{s}(i)$ values and the evaluation of the TSS_{within} values are retained as described above. As this can result in more than one set of initial centroids, the set that has the lowest TSS_{within} of the remaining sets is chosen as the final location of the initial centroids.

3.3. Analysis of monthly flood characteristics

3.3.1. Identification of flood dominant and flood scarce months

The k clusters obtained are then further analysed for their temporal flood occurrence characteristics, with the aim of identifying months in which floods occurred often and months in which floods happen seldom or never (hereafter termed flood dominant and flood scarce months, respectively). This classification into flood dominant and flood scarce months is achieved by a significance test in which the observed monthly flood occurrence is compared to the expected occurrence of a uniform flood seasonality distribution (1/12 of the floods are expected to occur in each month) (Cunderlik et al., 2004).

As the twelve months contain a different number of days, the monthly counts of flood occurrence c_i need to be modified to match a ‘30-day month’ to obtain adjusted monthly percentages of flood occurrences (\tilde{l}_i) that allow a direct comparison of the counts. \tilde{c}_i is the adjusted monthly count of flood occurrences with i being the months 1 to 12, and d_i the number of days in that month (February has 28.25 days to account for leap years).

$$\tilde{c}_i = c_i \cdot \frac{30}{d_i} \quad (8)$$

$$\tilde{n} = \sum_{i=1}^{12} \tilde{c}_i \quad (9)$$

$$\tilde{l}_i = \frac{\tilde{c}_i}{\tilde{n}} \cdot 100 \quad (10)$$

The one-sided 95% upper (L_{upper}^n) and lower (L_{lower}^n) confidence intervals are approximated following Cunderlik et al. (2004):

$$L_{upper}^n = \frac{n+11.491}{0.048 n^{1.131}} \quad (11)$$

$$5 \quad L_{lower}^n = \frac{n-27.832}{0.199 n^{0.964}} \quad (12)$$

with n being here the record length.

If the monthly percentage \tilde{l}_i of a given month is above or below the confidence interval, this month is considered to be either flood dominant or flood scarce respectively (at a 5% significance level). Only stations with least 30 years of data are analysed (3356), as the above approximation is only valid for records with at least 30 data points. The 563 stations with shorter records are excluded from the remaining analyses.

Depending on the record length, the upper and lower thresholds of the confidence interval vary. For example, for a 30-year long record, the L_{upper}^n and L_{lower}^n for \tilde{l}_i are 10.126% and 0.246% respectively (i.e. \tilde{c} counts of flood occurrences for a given month of 3.037 and 0.073), whereas for a 51-year long record the thresholds for \tilde{l}_i are 15.251% and 2.629% respectively (i.e. \tilde{c} counts for a given month of 7.778 and 1.341). The months that have their \tilde{l}_i within these thresholds are not further classified here. For each station independently, each month of the year is classified as flood dominant, flood scarce or neither of them (i.e. unclassified), based on the available record length.

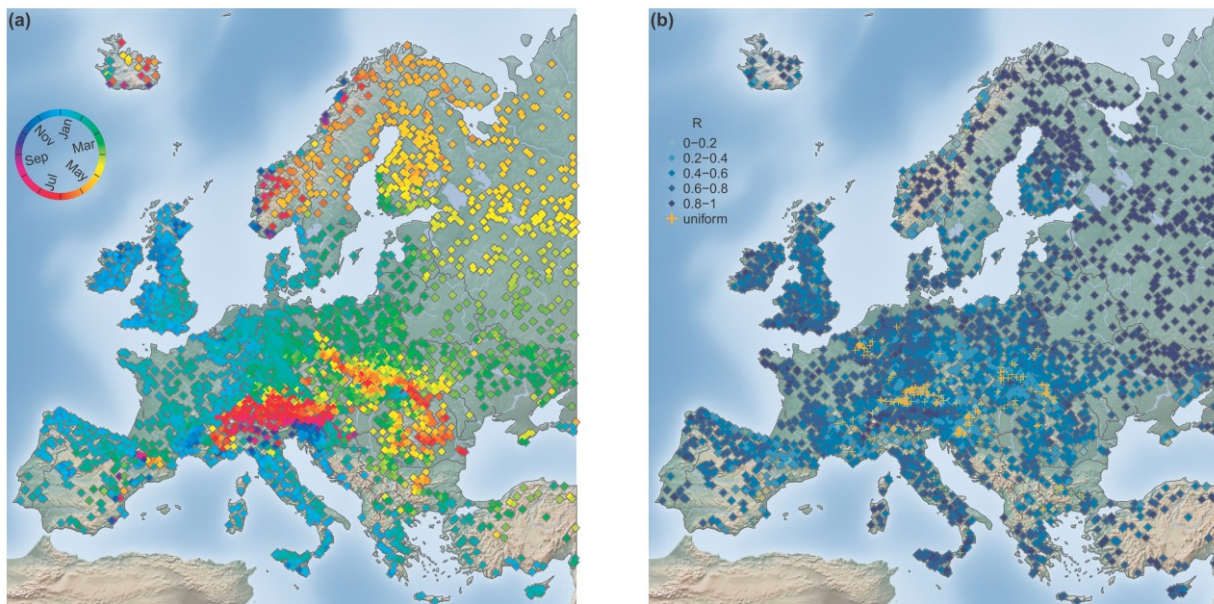
3.3.2. Identification of bimodal and unimodal flood seasonality distributions

Flood dominant or flood scarce periods for a station are obtained by segmenting the year based on the consecutive occurrence of months with the same classification (i.e. either flood dominant or flood scarce). If the adjacent months at the beginning and the end of the year belong to the same classification, the months are combined to form one consecutive period. The length of the flood dominant and flood scarce periods is determined by summing the number of months within each individual period. Based on these periods, the monthly flood seasonality distribution is identified as bimodal if two flood dominant periods, independent of their length (i.e. a minimum of one month each), are separated by at least one flood scarce month (before and after). A unimodal flood seasonality distribution is identified if all months (minimum of one month) considered as flood dominated occur consecutively.

4 Results

4.1 Flood Seasonality Analysis

Figure 4 shows the mean flood seasonality and the temporal concentration of flood occurrence within the year. A distinct spatial pattern of the mean timing of floods within the year can be observed (Fig. 4a). Below 60° latitude, the mean seasonality transitions from winter floods in the West to spring floods in the East due to increasing continentality. Stations located in mountainous areas (e.g. the Alps, the Carpathians, and the Pyrenees) exhibit predominately summer floods and disrupt this west to east transition of flood timing. Above 60° latitude, spring floods dominate the spatial pattern, except for coastal areas in which autumn and winter floods are observed. The temporal concentration of floods around the mean date of flood occurrence (R-value) (Fig. 4b) is highest in north-eastern Europe. High temporal concentration is also apparent at the western coast of Europe except for the western coasts in northern Europe where floods are spread more evenly throughout the year. Catchments on the foothills of mountainous areas (e.g. around the Alps and the Carpathians) also tend to have smaller R-values and sometimes exhibit a uniform occurrence of floods throughout the year. The orange crosses in Fig. 4b indicate the stations for which circular uniformity could not be rejected at a significance level of $\alpha=0.01$. The characteristics of stations with uniform flood occurrence are later examined in detail (see Fig. 6).



15 **Figure 4. Seasonality of floods in Europe for 1960-2010. Mean date of flood occurrence \bar{D} (a). Flood Concentration Index R (b); Stations with circular uniformity (186 stations) are marked by orange crosses. In both panels, $n=4105$ stations.**

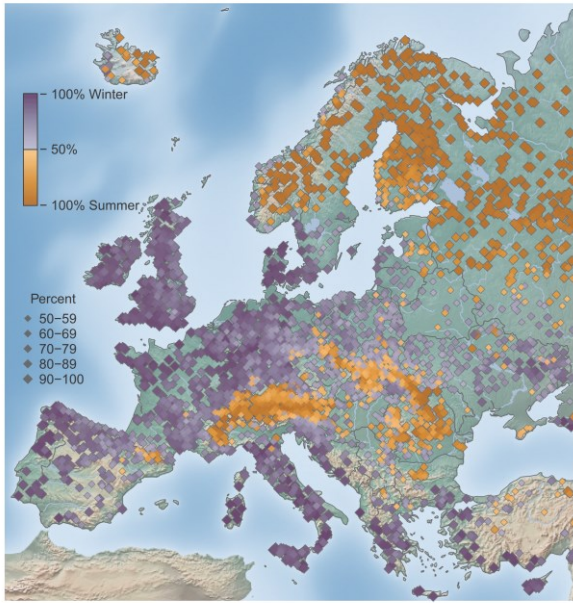


Figure 5. Percentage of winter half-year (October to March) and summer half-year (April to September) floods. Dark purple or orange colours indicate dominance of the winter or summer half year respectively; light colours indicate an almost equal occurrence in the two half-years. $n=4105$ stations.

- 5 An alternative way of examining the flood seasonality is the frequency of floods occurring in the winter and summer half years (Fig. 5). The winter and the summer half-years are defined as October-March and April-September, respectively. There is a clear dominance of summer floods in mountain ranges (e.g. Pyrenees, Alps, and Carpathians) and in the northern and north-eastern parts of Europe, which can be characterised by a continental climate. In the rest of Europe, floods predominately occur in the winter half-year. Transitional areas, for which no clear seasonal distinction can be made (< 60 % of either winter
- 10 of summer half-year floods), can be found in and around Poland, Lithuania, Belarus and parts of the Ukraine. In these transitional areas, no half-year flood season dominates, as the AMF of these stations tend to occur in March and April around the cut off date separating the winter- versus summer half-years. Additionally, a less well-defined flood seasonality can be found on the foothills of mountains, where both winter and summer floods occur (mixed distribution), depending on whether floods are snowmelt induced, summer rainfall induced, or the floods are uniformly distributed around the year.
- 15 In order to further examine the relationship between week seasonality (low R-values) and uniform flood occurrence, the spatial location of the stations for which circular uniformity could not be rejected (at a significance level of $\alpha=0.01$) is shown in Fig. 4b. The stations with a uniform flood seasonality distribution are found predominately at low to medium high altitudes (< 1000 m) (Fig. 6a) and in small catchments (Fig. 6b). However, for some of the stations with a small Flood Concentration Index R, uniformity could not be rejected for the significance level $\alpha=0.01$, which reveals that small R-values do not

necessarily indicate uniformity. These stations possess a skewed or a bimodal distribution of flood occurrence throughout the year.

For the European continent, stations with high elevation tend to have a high Flood Concentration Index R and occur mainly in early summer (mean seasonality in May and June) (Fig. 6a). At higher elevations, there are no stations with uniform flood occurrence, whereas at lower elevations (< 1000 m) uniform distributions do exist. In Figure 6b, uniformity cannot be rejected for catchments of all sizes (note: 115 catchments with missing catchment area are not shown). Larger catchments tend to have a few stations with a Flood Concentration Index < 0.2 , most of which can be considered of having a uniform distribution, whereas catchments with less than 1000 km² exhibit more often smaller R -values and these tend to have uniform distributions (Fig. 6b). Overall, uniformity of flood occurrence seems to be predominately conditioned by geographical location (foothills of mountains) (Fig. 2b). Hydrological stations near mountainous areas tend to have a lower catchment elevation and smaller catchment area.

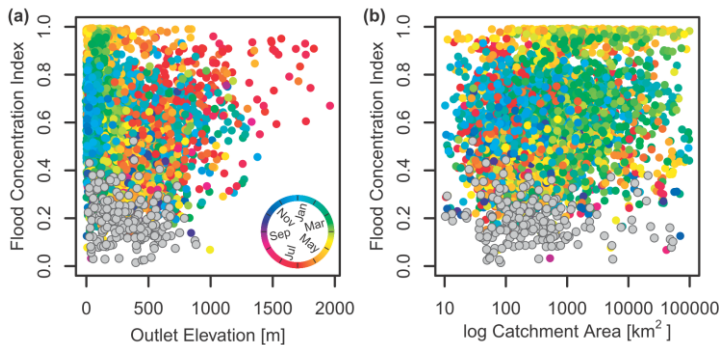


Figure 6. Flood Concentration Index R of floods in Europe (1960-2010) dependent on station elevation, $n=4105$. (a) and catchment area, $n=3900$. (b). Colour of points indicates the mean timing of floods (\bar{D}) at that hydrometric station location. Grey points indicate the 186 stations for which circular uniformity could not be rejected ($\alpha=0.1$).

15

The mean frequency of floods in each season (based on individual flood events) is shown in Fig. 7 (for all 3919 stations for which the null hypothesis of circular uniformity was be rejected; $\alpha=0.1$). Floods occurring between January and March are classified as winter floods, spring floods occur between April and June, summer floods between July and September, and autumn floods between October and December. Figure 7a, displays an increase in the mean frequency of summer floods with increasing elevation and conversely a tendency towards decreases in the frequency of autumn and winter floods due to the increasing dominance of summer floods (see also Fig. 6a). Autumn floods have the highest frequency in most of the elevation ranges analysed. In two elevations ranges (91 to 125 m and > 440 m), spring floods have the highest occurrence frequency. Figures 4a and Fig. 5, suggest that the high mean frequency of spring floods occurs either in catchments with intermediate elevation in north-eastern Europe or in, or around, mountainous areas (flood timing is often towards the end of June, close to July which is the first month used for the classification of summer floods).

25

Smaller catchments in Europe are more similar regarding their mean frequency of seasonal floods (Fig. 7b, note: 115 catchments with unknown catchment area are not shown). With increasing catchment area, the percentage of spring floods increases. This observed tendency is related to the uneven spatial distribution of larger catchments in the database (Fig. 2b). Stations with large catchment areas can be found predominately in central and eastern to north-eastern parts of Europe, which are dominated by spring floods.

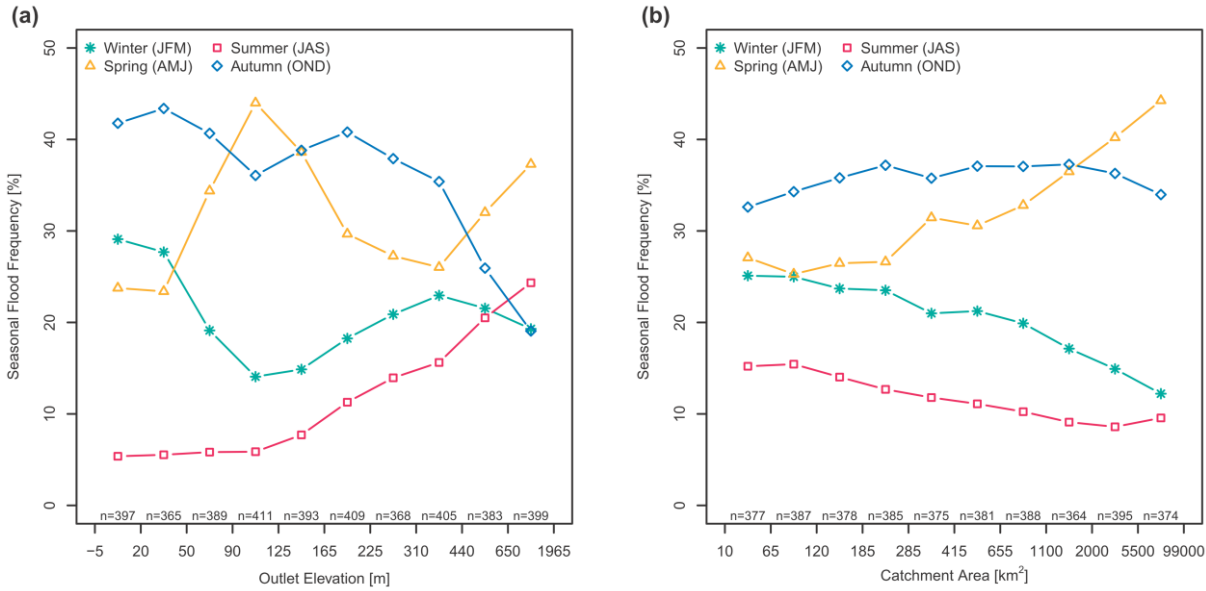


Figure 7. Mean frequency of seasonal floods by ranges of outlet elevation $n=3919$ (a) and catchment area $n=3804$ (b). In both panels, the ranges on the x-axis were selected so that roughly an equal number of stations is allocated to each range. In both panels, stations with a uniform distribution excluded.

4.2 Cluster Analysis on Flood Seasons

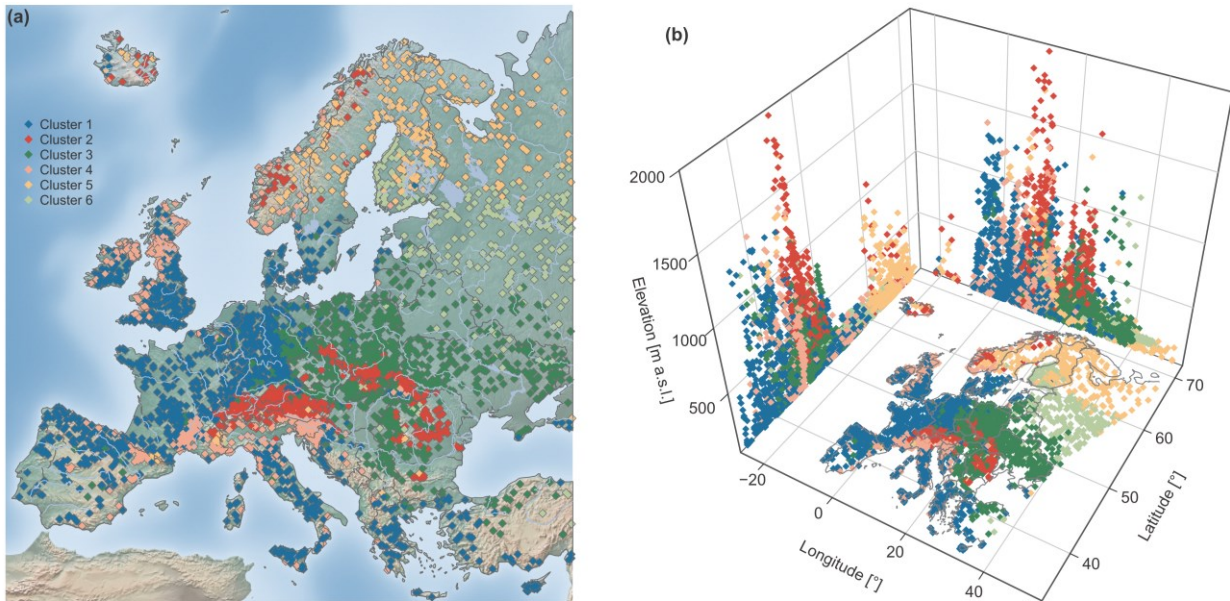
In the previous section, the strong influence of the geographical location on the timing of flood occurrence at a given station is apparent. Therefore, it is of interest to identify larger scale regions in Europe with relatively similar seasonal flood occurrence. These regions are identified with the help of cluster analysis after the best possible initial centroid locations are determined. Table 1 summarises the sensitivity of the location of the initial centroids and shows the percentage of how often a specific number of clusters ($5 \leq k \leq 7$) obtained the highest mean silhouette value $\bar{s}(i)$ from the 10,000 random initial cluster centroids and the highest overall $\bar{s}(i)$ value. The Table indicates that, with the same initial centroid placement for 5, 6 or 7 clusters (same as 5 clusters plus one or two additional initial centroids for 6 and 7 clusters respectively), 46% of the random samples generated the highest $\bar{s}(i)$ values for $k=6$ clusters. Additionally, the six initial cluster centroids result in clusters that obtain the maximum $\bar{s}(i)$ of 0.443 for all 10,000 random initialisations. In the initialisations for which 5 or 7 clusters obtain the highest $\bar{s}(i)$, the maximum $\bar{s}(i)$ are always lower than the maximum that is obtained with 6 clusters. Therefore, the sets of initial centroid locations that obtain the highest $\bar{s}(i)$ of all random initialisations (0.443) for $k=6$ are chosen as candidates for

further selection of the initial centroid position. From these only the sets of initial locations are retained, for which the Elbow method (based the reduction in the total within cluster sum of squares (TSS_{within})) also results in $k=6$ optimal clusters. As several sets with different initial centroid locations fulfil this criterion, the initial set of centroids that yields the lowest TSS_{within} for $k=6$ is selected and is used in the remainder of the study.

5 **Table 1. Number of clusters and average silhouette value $\bar{s}(t)$ for 10,000 random initial cluster centroids.**

Number of clusters (k)	Samples with highest $\bar{s}(t)$	Maximum average value $\bar{s}(t)$
5	39 %	0.438
6	46 %	0.443
7	15 %	0.396

Figure 8 depicts the spatial distribution of the six clusters of monthly flood occurrences obtained using the methodology described above. Most clusters are spatially coherent except Cluster 4. Table 2 and Fig. 9 assist in interpreting these clusters. Cluster 1 is located in western, central and southern Europe and contains most of the stations (~36%). The mountainous regions in Europe (highest average outlet elevation), the Alps and the Carpathian and Scandinavian Mountains, in Cluster 2 account for ~15% of the stations. Most stations, located in central and eastern Europe up to 55°N (~24%), are assigned to Cluster 3. Cluster 5 and 6, located predominately in northern and north-eastern Europe, are the two smallest clusters containing ~8% and ~6% of all stations respectively. Most of stations assigned to Cluster 6 are located above 60°N and are low lying.



15 **Figure 8. Spatial distribution of the six clusters of monthly flood frequencies (a), $n=3919$ stations. The vertical axes of the panel on the right shows the catchment outlet elevation (b) $n=3804$ stations.**

Table 2. The six clusters of monthly flood frequencies in Europe and their characteristics.

Number of cluster (<i>k</i>)	Location	Number of stations	Average silhouette width $\bar{s}(i)$	Average station elevation [m a.s.l.]	Average catchment area [km ²]	Average of all D_i (DOY)	R-value over all D_i
1	Western, Central and Southern Europe	1427	0.51	220.9	2193.0	25 January (25)	0.60
2	Mountainous regions	595	0.40	538.8	2010.1	30 June (181)	0.53
3	Central and Eastern Europe	934	0.37	207.6	3950.8	22 March (81)	0.51
4	Western British-Irish Isles, Western Coast of Norway and Northern Mediterranean	405	0.26	263.8	1757.9	5 December (339)	0.36
5	Northern Europe	307	0.56	204.9	3940.4	19 May (139)	0.85
6	North-Eastern Europe	251	0.62	126.2	6607.4	15 April (105)	0.84

Cluster 1, 5 and 6 are well defined (i.e. high within-cluster similarity or average silhouette width $\bar{s}(i)$). Cluster 4 is the least well-defined cluster in terms of $\bar{s}(i)$ and also in terms of spatial coherence. The stations in Cluster 4 are found in several regions of Europe (western British-Irish Isles, western Coast of Norway and northern Mediterranean). Cluster 4 has the smallest average catchment area and the highest spread of flood occurrence around the mean date of flood occurrence (early December) (see also ‘mean of all’ in Fig. 10). The largest catchment areas are found in northern and north-eastern Europe (Cluster 3, 5 and 6). The average dates of the flood timing (D_i) in Clusters 5 and Cluster 6 are mid-May and mid-April, respectively, with all floods being highly concentrated around the average date. Cluster 1 is also strongly seasonal with a mean flood occurrence in late January, whereas the mountainous areas (Cluster 2) have their mean flood occurrence in summer.

Overall, the geographical location seems to determine the membership of a cluster, although the geographic location is not included as a variable for clustering. Few stations that do not fit the large-scale, coherent cluster pattern (i.e. spatial outliers).

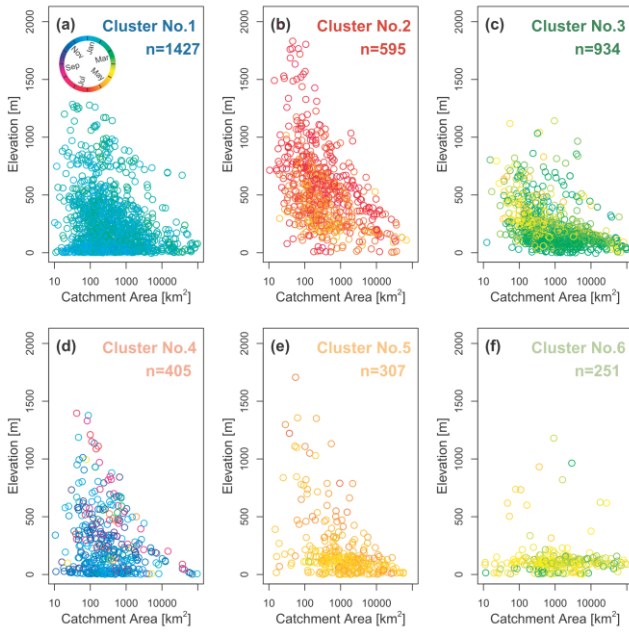


Figure 9. Mean flood seasonality (\bar{D}) as a function of catchment outlet elevation [m a.s.l.] and catchment area [km²] grouped by the six clusters. Colour of the points in all panels indicates the mean timing of floods at that hydrometric station. Total number of stations in the analysis is: 3919; in each panel n denotes the number of stations assigned to a specific cluster (in panel (a)-(f) there are 115 stations (69, 4, 19, 14, 3, and 6 stations respectively) not being displayed due to unknown catchment area).

5

Figure 10 shows the mean flood seasonality (\bar{D}) for each station, the overall mean seasonality of all floods belonging to the same cluster and the mean of all mean flood seasonalities, together with the respective temporal concentration around these means. The stations within their respective clusters display similar concentrations, as indicated by R-values >0.9 of the mean of the cluster mean flood seasonalities (large points with crosses). The exception is Cluster 4, which has the lowest temporal concentration of the mean floods with R=0.71. In this cluster, the temporal concentrations of the floods of the individual stations are lower than those of the stations in the other clusters. The R-values of the mean of all AMF (large points) in both Clusters 5 and Cluster 6 (R=0.85 and R=0.84, respectively) are close to the mean of all mean seasonalities. This indicates that, in these clusters, not only the mean seasonalities (\bar{D}) are temporally concentrated but also the individual floods (D_i). The mean seasonalities of most of the stations assigned to these clusters have a strong temporal concentration around their regional mean (high R-value), and only a few stations have a larger spread around the mean date of flood occurrence. The R-values of the regional mean seasonality of all AMF in the other clusters are much smaller than the R-values of the mean of all mean seasonalities. This indicates that the clustering algorithm performs well with regard to clustering stations that have a similar mean seasonality, but individual flood events may exhibit higher temporal variability.

20

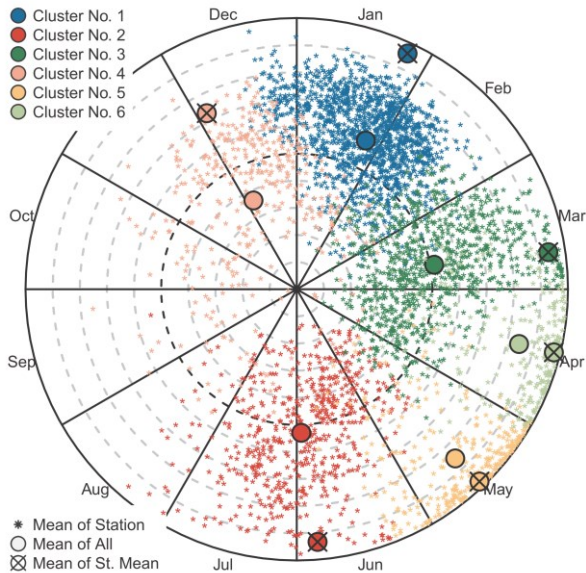


Figure 10. Mean Seasonality and temporal concentration of floods for each station (small points), the mean over all floods within specific clusters (large points) and the mean of all mean flood seasonalities (large points with crosses) within specific clusters. Colours correspond to clusters. Distance to centre is a measure of the temporal Flood Concentration Index R , with the centre corresponding to $R=0$, the black dashed circle to $R=0.5$ and the outer full circle to $R=1$. The grey dashed circles correspond to intervals of $0.1 R$. Total number of stations: $n=3919$.

The mean flood seasonality for both stations and clusters has limited information content, as it only reflects the first moment of the seasonality distribution. Therefore, it is of interest to examine the full monthly flood distribution. Theoretically, if all floods were equally spread over the year, all months would contain $8.\bar{3}\%$ of all the AMF. Figure 11 shows the relative monthly frequency of AMF of the cluster centroids (CC) (i.e. the respective cluster means). All CC have at least one month, in which more than 18% of the annual maximum floods occur. This indicates that in each of the CC there is a clear dominant month for floods to occur and therefore clear flood distinct flood seasonality. The CC of Cluster 5 and Cluster 6 in northern and north-eastern Europe have the most pronounced flood seasonality, where a single month (May and April, respectively) contains $>65\%$ of the AMF. For both CC the months before and after this peak account for $\sim 10\%$ and $\sim 15\%$, respectively, with the remaining months containing less than 3% of the AMF. CC 1 (western and southern Europe) and CC 2 (mountainous regions) exhibit an almost bell-shaped distribution with the AMFs peaking in the winter and summer half of the year, respectively. CC 3 (central and eastern Europe) peaks at the beginning of the year (strongest peak in March, 28%) with less than 10% if AMFs in the rest of the year. CC 4 is the cluster with the least pronounced peak in the monthly flood frequencies.

There is a small peak of flood occurrences in the winter months (October to September, each month <20%) and a low flood season in the summer months.

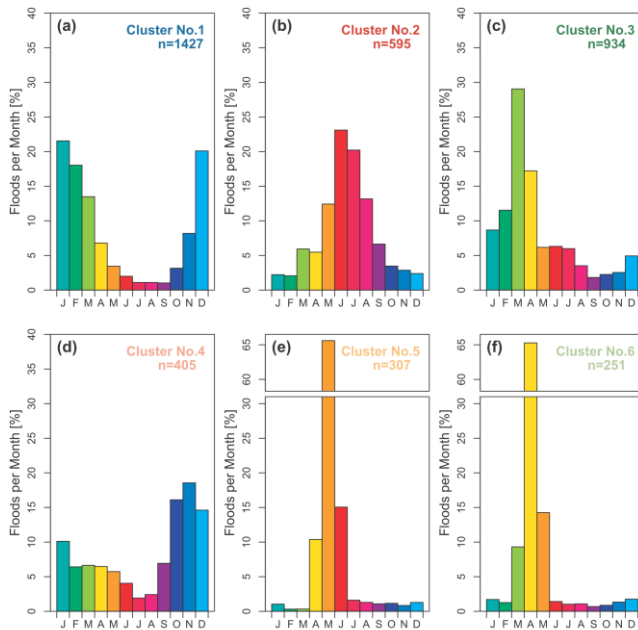


Figure 11. Frequency of occurrence of maximum annual floods by month for the cluster centroids CC (i.e. cluster means). Total number of stations: $n=3919$; in each panel n denotes the number of stations assigned to a specific cluster.

Figure 12 depicts the full range of relative monthly flood frequencies of all stations assigned to each cluster, to allow an in-depth interpretation of the results beyond the cluster mean (i.e. CC). The shape of the monthly flood seasonality distribution of the medians of each cluster (i.e. monthly percentages) resembles the shape of the cluster centroids in Fig. 11 for most clusters. Differences in the shape of the distributions are mainly caused by stations that contain months with a deviating frequency of AMF.

In Cluster 1, the shape of the distribution remains similar, however for individual stations (outliers) the winter months have a much higher percentage of flood occurrences (up to 55%), the summer months stay below 15% of the AMF (Fig12a). In Cluster 2, June and July remain the months with the highest percentages. For some stations, August, and to a lesser extent May, are the most important months (Fig. 12b). This characteristic could not have been detected when examining the CC in Fig. 11b) alone. October to February remain months with low flood occurrences. Within Cluster 3, March and April stand out as the most important months of flooding, as it already seen in Fig. 11c). However, it becomes visible now that these months have the highest spread between stations, while the other months have a much smaller spread (Fig. 12c). In Cluster 4, the CC show frequent floods in October to January (Fig 11d). However, when taking into account the full range of all the stations, the months April, May, and June also contain a high percentage of AMF (up to 55 %) for individual stations (Fig.12d). This

characteristic is not detectable in neither the CC nor the median of the cluster and indicates that, for some stations (i.e. locally) these months are very important in terms of flooding. The appearance of months with an additional secondary peak in flood occurrence indicates the possible existence of a bimodal distribution for several stations. The medians and all stations of Cluster 5 and Cluster 6 exhibit a high occurrence of flooding in May and April, respectively, as it was already detectable in Fig. 11. Most other months of the year show very low frequencies for the median with a very low spread between stations. The exceptions are the months immediately before and after the main flood month, which can have high percentages of flooding for individual stations as well (Fig. 12). This high concentration of floods around a single month is the reason for the stations, belonging to these two clusters, to show very high R-values in Fig. 4b.

In summary, when taking all stations within a cluster into account, one can see that the characteristics that are present in the monthly distributions of the CC are retained. However, some additional characteristics such as the emergence of a bimodal distribution in Cluster 4, which was smoothed-out in the CC or additional months with higher relative monthly flood frequencies and outliers, can be identified.

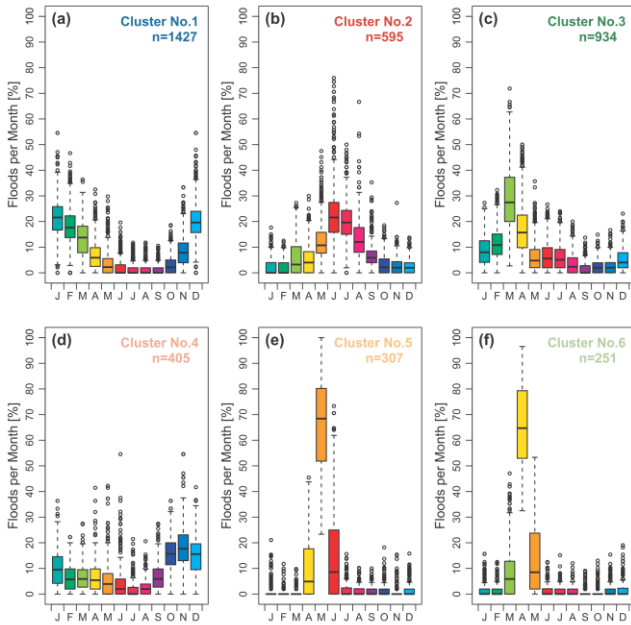


Figure 12. Boxplot of the percentage of floods per month for each station, grouped by cluster (a-f). The top and bottom of the boxes show the 75th and 25th percentiles (i.e. the upper and lower quartiles) respectively, whiskers extend to $1.5 \times$ interquartile range beyond the box, the black band indicates the median, and outliers are shown as points. Total number of stations: $n=3919$; in each panel n denotes the number of stations assigned to a specific cluster.

To investigate further the possible existence of a bimodal seasonality distribution, the classification into flood dominant and flood scarce months is performed (see Section 3.3.1.), on records with more than 30 years of data (n_{sub}). Each cluster has more than 80% of their stations with series longer than 30 years (see Table 3 for the exact numbers).

Figure 13 shows the percentages of stations in each cluster for which a specific month can be considered, statistically significant ($\alpha=0.05$), as being flood dominant or scarce. In Cluster 5 and Cluster 6, the months May and April respectively are classified as flood dominant for 100% of the stations. There are four clusters with at least one month that can be considered not to be flood dominated for 100% of the station (marked by stars above the x-axis in Fig. 13). In Cluster 1, this is the month June and September, in Cluster 3, September, in Cluster 5, February and March, and August to October and in Cluster 6, August to November. In all clusters, there is not a single month, for which all stations would exhibit flood scarcity (i.e. 100%). 5 out of 6 clusters (apart from Cluster 2) have at least one month that can be considered not to be flood scarce for 100% of the station (marked by stars below the x-axis in Fig. 13). This is February for Cluster 1, March for Cluster 3, October and November for Cluster 4 and March for Cluster 5 and Cluster 6 respectively. Based on the percent of stations that have flood dominance, there is again an indication in Cluster 4 that some of the stations might have a bimodal distribution with a primary peak in winter, and a secondary peak in April and May, with 12.01% and 10.21% of the stations have a significant flood dominated month respectively.

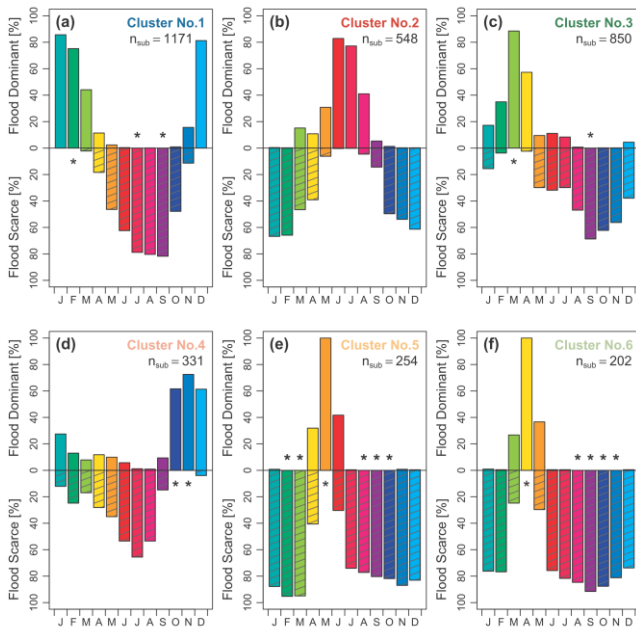


Figure 13. Percent of stations with months that can be considered significantly ($\alpha=0.05$) flood dominant (upward bars) or flood scarce (downward shaded bars) grouped by cluster (a-f). Months for which no station showed significance in the respective category are marked with a star. Total number of stations with records >30years: $n_{sub}=3356$. In each panel, n_{sub} indicates the number of stations assigned to a specific cluster.

20

Figure 14 shows the maximum and minimum duration (in months) for flood dominant (a and b) and scarce (c and d) periods respectively. In each panel, the percentages are listed for each cluster separately.

There is a very small number of stations (<1%) in Clusters 1, 2 and 4 for which no significant flood dominant season could be identified (i.e. 3, 2 and 2 stations, respectively) (Fig. 14a). This means that the floods are not uniformly distributed throughout the year (as stations for which uniformity could not be rejected were already removed from this dataset in a previous step), but the number of floods per months does not cross the L_{upper}^n threshold for the months to be classified as flood dominant. All clusters contain stations that have a maximum of five consecutive flood dominant months, with exception of Cluster 6, which has one station that has six consecutive months (Fig. 14a). Most of the stations have a maximum length of two consecutive months apart from Cluster 1, which has the highest number of stations with three consecutive months (Fig. 14a). All stations in Clusters 5 and 6 have at least one flood scarce month. In all other clusters, < 5% of the stations have no flood scarce month (Fig. 14c and d), i.e. most of the stations have a minimum duration of 1 flood scarce month (Fig. 14d). This is important, as the existence of flood scarce month is a necessary condition for the identification of bimodal flood seasonality distributions in the next part of the analysis. Most of the stations in Cluster 5 and 6 have the same maximum and minimum duration of 2 months when considering the flood dominant months (Fig. 14a and b) and also the same number of maximum and minimum length of flood scarce months between 9 and 10 months (Fig. 14c and d). This indicates that the seasonal flood seasonality distributions are likely unimodal.

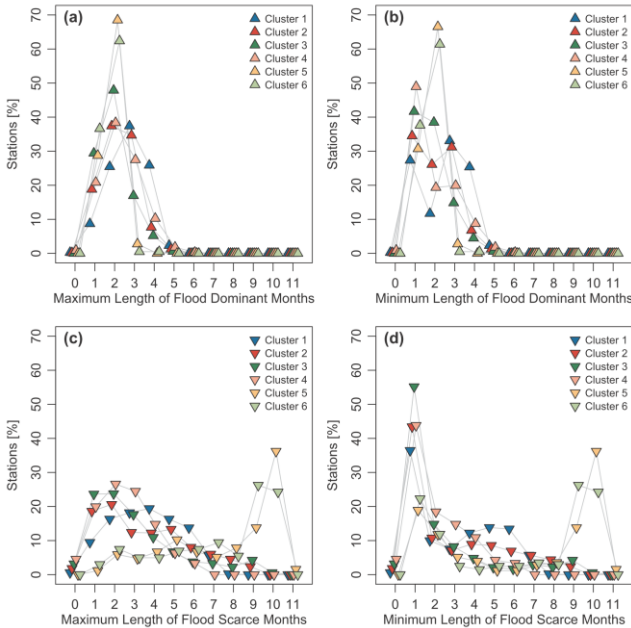


Figure 14. Percent of stations within the same consecutive monthly flood classification, grouped per cluster. The x-axes show the maximum (left panels) and minimum number (right panels) of consecutive months classified as flood dominant (upper row) and flood scarce (lower row). Total number of stations with records >30years: $n_{sub}=3356$.

Based on the alternating occurrence of flood dominant and flood scare months the flood seasonality distributions of 79 stations are classified as bimodal. 2490 stations have a unimodal seasonality distribution due to the uninterrupted occurrence of the flood dominant months (Table 3).

- 5 Cluster 4 has the highest number of stations (29) and the highest percentage of stations (~9 %) with bimodal distributions. Cluster 4 has also the highest percentage of stations without a clearly defined flood seasonality distribution (~36%) and the lowest number of unimodal stations (~56%). This indicates that Cluster 4 is the cluster with the most diverse flood seasonality distributions, which is consistent with its low average silhouette values detected before. In Cluster 2 and Cluster 3, 20 and 24 stations are classified as bimodal, the other clusters contain less than 5 bimodal stations.

10

Table 3. Six clusters and their characteristic flood seasonality distributions, based on the subset of station with records > 30 yrs.

No. of <i>k</i> cluster	Location	No. Stations > 30 years	Bimodal		Unimodal		Undefined		Primary Flood Season	Secondary Flood Season*
			No.	[%]	No.	[%]	No.	[%]		
1	Western, Central and Southern Europe	1171	1	0.09	861	73.53	309	26.39	Dec to Mar	-
2	Mountainous regions	548	20	3.65	393	71.72	135	24.64	May to Aug	Mar
3	Central and Eastern Europe	850	24	2.82	604	71.06	222	26.12	Feb to Apr	Jun & July
4	Western British-Irish Isles, Western Coast of Norway and Northern Mediterranean	331	29	8.76	184	55.59	118	35.65	Oct to Jan	May
5	Northern Europe	254	4	1.57	249	98.03	1	0.39	May & Jun	-
6	North-Eastern Europe	202	1	0.50	199	98.51	2	0.99	Apr	-
All	Europe	3356	79	2.35	2490	74.2	787	23.45	-	-

*Only for bimodal flood seasonality distributions in clusters with at least 20 stations.

- 15 Primary and secondary flood seasons are identified, for each cluster separately, if the median of the monthly flood percentage is >8.33% (1/12). Primary flood seasons are based on all stations with at least 30 years and secondary flood seasons are identified from the bimodal flood seasonality distributions, from cluster with at least 5 bimodal stations (excluding the months that are already included in the primary flood season) (Table 3).

- 20 In Figure 15, the monthly bimodal, unclassified and unimodal flood seasonality distributions are shown for each cluster separately. In Cluster 1, 74% of the stations have unimodal flood distributions and one stations is classified as bimodal. The other stations have an unclassified seasonality distribution, which is mainly due to the absence of an additional month classified as either flood dominant or flood scare. Cluster 2, Clusters 3 and Cluster 4 show a monthly seasonality distribution with a distinct secondary flood season (Fig. 15.b.1 to 15.d.1). In the mountainous regions (Cluster 2), the secondary peak in the bimodal flood seasonality distribution in March precedes the main flood season in summer. In central and eastern Europe (Cluster 3) the main flood season in February to April is followed by secondary flood in June and July. In Cluster 4, the primary flood season in October to January is followed by an additional month of flooding in May. 98% of the stations in
25 Cluster 5 and Cluster 6 in northern and north-eastern Europe are classified as unimodal.

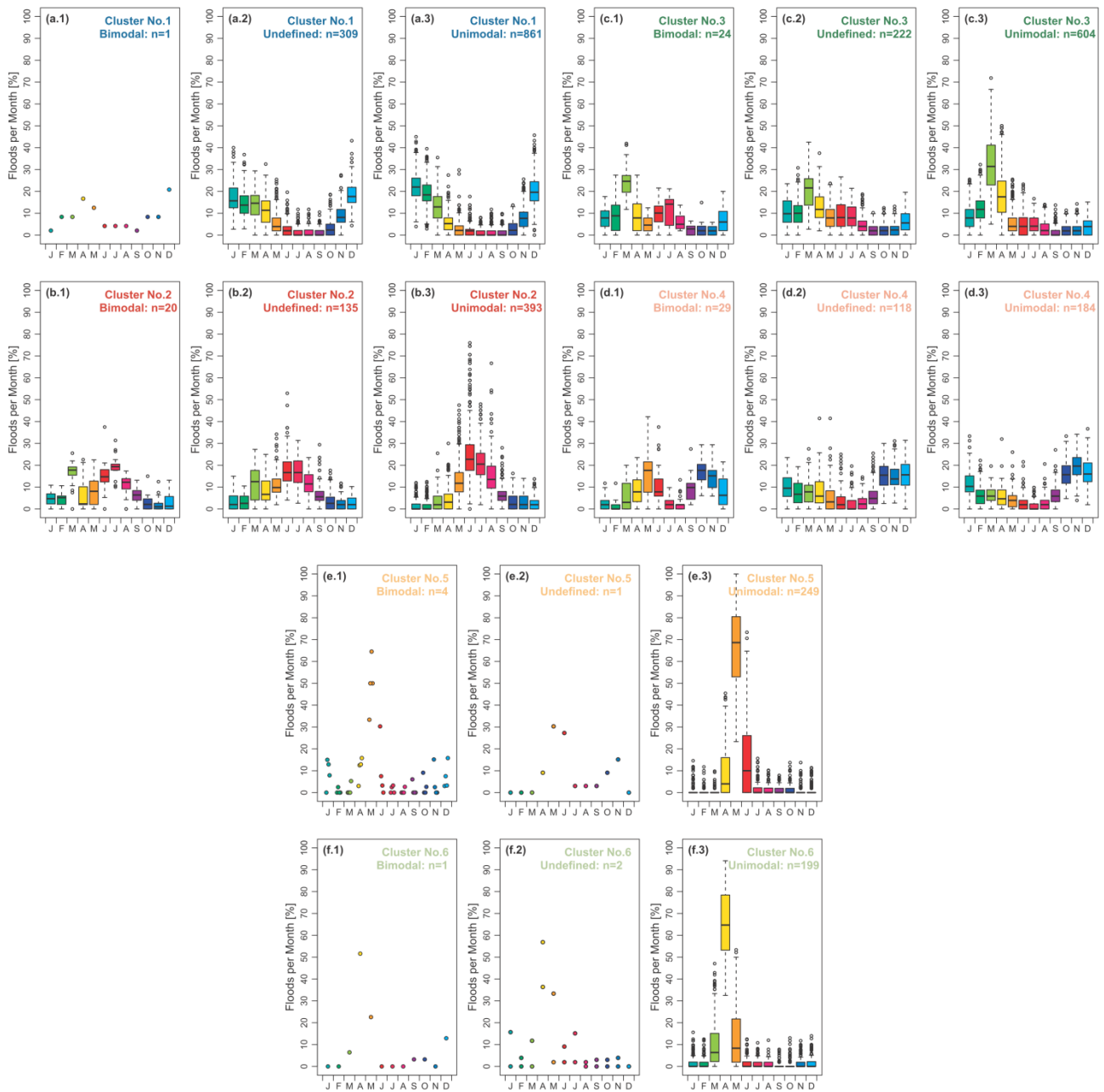


Figure 15. Boxplot of the percentage of floods per month for each station of all stations with at least 30 years of data, grouped by their cluster (a-f) and by their annual flood seasonality distribution being bimodal, undefined or unimodal (x.1 - x.3 respectively). The top and bottom of the boxes show the 75th and 25th percentiles (i.e. the upper and lower quartiles) respectively, whiskers extend to $1.5 \times$ interquartile range beyond the box, the black band indicates the median, and outliers are shown as points. Panels containing less than 5 stations show points instead of boxplots. Number of stations: $n_{sub}=3356$. n denotes the number of stations within each flood distribution classification.

Figure 16 shows the spatial pattern of the stations with a clear bimodal or unimodal seasonality distribution. For most of the bimodal stations the R-value is low (mean R-value of all bimodal stations is 0.35) (Fig. 16a). However, bimodality does not necessarily imply a low concentration around the mean. If, for instance, the two flood seasons are separated by only one flood scarce month the R-value can be high. The station with the highest R-value of all bimodal stations ($R=0.73$) is located in Finland (Cluster 5), for which the secondary flood season occurs just 2 months before the primary flood season. Even though bimodality in the flood seasonality distribution is only detected in a small number of stations, the locations of these stations are not randomly distributed across Europe, but rather located in close spatial proximity in certain regions.

In northern and eastern Europe (Cluster 5 and Cluster 6), the duration of the period of flood dominant months (unimodal seasonality distribution) is the shortest (Fig. 16b) and lasts, on average 1.73 and 1.65 months, respectively. The stations with a unimodal flood seasonality distribution in Cluster 1 have, on average, the longest period duration (~3.2 months). In Cluster 2, Cluster 3 and Cluster 4 the periods of flood dominant months last, on average, 2.57, 2.16 and 2.65 months respectively.

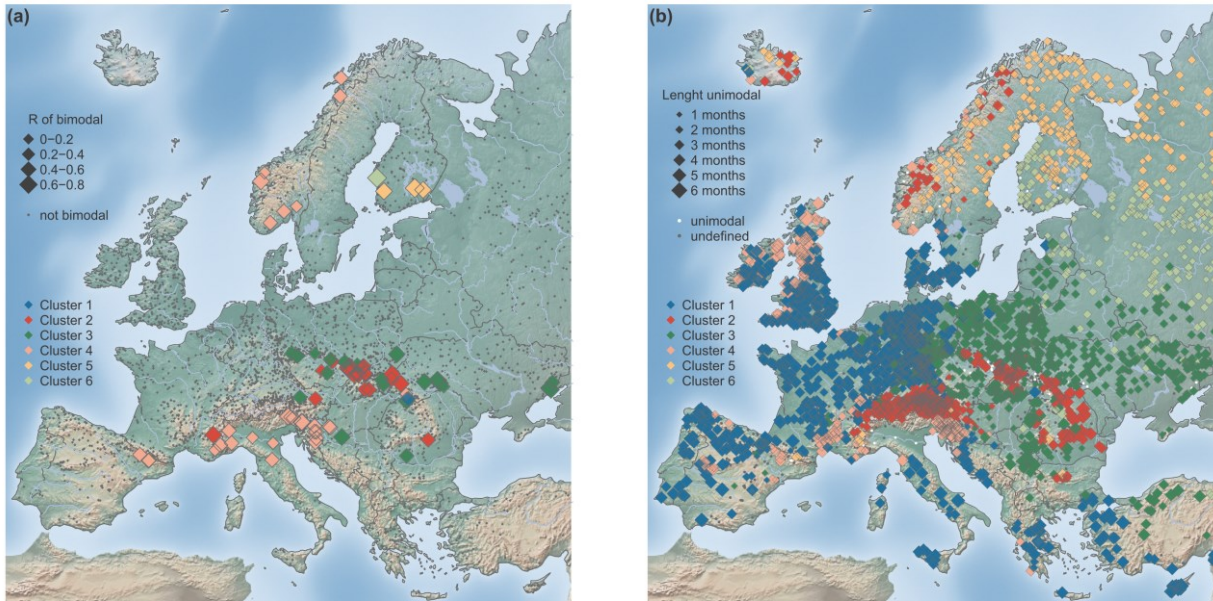


Figure 16. Spatial distribution of the stations with bimodal flood seasonality distributions ($n=79$) with the point size scaled by concentration R (a), and stations with unimodal distributions ($n=2490$) with the point size scaled by the length of the flood dominant period (b).

5 Discussion

This study provides a detailed analysis of the seasonality characteristics of annual maximum floods in Europe. While previous studies analysed the mean flood seasonality at national or regional scale, this paper aims at identifying large-scale geographical regions with similar temporal flood characteristics and to describe these regions in detail.

5 Previous studies in the US (e.g. Lecce (2000)) have suggested that catchment area has a strong effect on the flood seasonality (higher frequency in summer and autumn due to short duration summer storms of limited areal coverage). In Europe, this does not seem to be the case. Smaller catchments show little difference in their flood seasonality when compared to larger catchments. Here a difference is only apparent in summer floods, which is apparent for the larger catchments located in eastern Europe. From the results obtained one can conclude that in Europe the station elevation (i.e. the catchment outlet
10 elevation), or the catchment area explains the timing of the flood occurrence to a lesser degree than geographical location. It would have been interesting to investigate if the catchment mean or maximum elevation would correlate better with the observed flood seasonality patterns and clusters, however, this information was only available for few of the stations and could be analysed if such information becomes available.

The clustering was performed on the monthly frequency of the AMF occurrence to obtain homogenous regions. Even without
15 considering the geographical location in the clustering, larger-scale spatial coherent clusters emerged that had distinct characteristics with regard to their flood seasonality distributions. The spatial seasonality patterns detected are similar to those of smaller scale studies (some of which use different methods). For example, the clusters detected in this study had similar spatial boundaries as the 3 clusters identified by Beurton and Thielen (2009) in Germany. Cunderlik et al. (2004) detected 3 regions with different flood seasonality in Great Britain, whereas this study identified 2 clusters. Their region with a high
20 number of floods in November (flood type 1) corresponds approximately to Cluster 4 identified in this study and their flood type 3 (floods occurring on average in January) corresponds to Cluster 1. They considered flood type 2 a transitional type between type 1 and type 3, which is included in Cluster 1 of in study. However, differences between local scale and continental scale analyses are expected, as the differences in the monthly flood frequencies that appear to be important at a smaller scale may be of less importance at a larger scale where larger differences in the monthly flood seasonality
25 distributions exist due to the existence of a larger variety of flood generation processes.

Based on the mean flood seasonality, the temporal concentration of the AMF around the mean timing and the geographical location on the map, one can hypothesise the causes behind the observed patterns. For example, Cluster 5 and Cluster 6 in eastern and north-eastern Europe are likely to be predominately driven by snow melt processes (Blöschl et al., 2017), which result in a high temporal concentration within a month due to the relatively fast melting of the snow once the temperatures
30 rise in the spring. Compared to Cluster 5 and Cluster 6, Cluster 3 is located further to the south and the west. These locations are marked by earlier snowmelt and a stronger maritime influence, which cause the floods to occur earlier in the year and exhibit a stronger influence of winter precipitation. For Cluster 2, which is primarily located in and around mountainous regions, one can infer that the AMF are caused by both snow and glacier-melt in the summer, and by heavy summer

precipitation, occurring in the summer months. In the coastal stations with strong maritime influence, located in Cluster 1, station elevation has little influence on the temporal occurrence of the annual maximum floods, as snow accumulation and melt is scarce. Therefore, this cluster can be considered to be mainly driven by extreme precipitation in late winter and early spring (see also Blöschl et al., 2017).

5 Cluster 4 is the most geographically dispersed cluster of all. The stations of Cluster 4 are located at the western coast of the British-Irish Isles, the western coast of Norway and the northern coasts of the Mediterranean. The temporal distribution of the AMF within the year shows a bimodal distribution for ~9% of the stations in this cluster. The floods can be considered to be predominately driven by late autumn and early winter precipitation (primary flood season), but also contain some floods caused by spring and early summer precipitation (secondary flood season).

10 In this study, only the annual maximum floods were available, but if more than one flood per year would be analysed (e.g. using partial duration series) the number of stations with bimodal distributions would probably be higher, as secondary flood maxima occurring in a year would also be included.

The detailed spatial and temporal flood seasonality information obtained in this study is important for practical applications such as farming operations, fluvial ecosystem management, water management (reservoirs and dams), hydropower production, flood protection policy and regional flood frequency analysis (Barnett et al., 2005; Blöschl et al., 2017; Klaus et al., 2016; Köplin et al., 2014; Ryberg et al., 2016), particularly for regions in which only limited information existed so far. Additionally, knowledge of the existence of these large-scale flood seasonality characteristics provides an important baseline for future research on floods in Europe. For example, the flood seasonality patterns can be used as an additional metric to test large-scale hydrological models for their ability to reproduce the spatial and temporal flood characteristics.

15 Moreover, the detailed assessment based on monthly flood occurrence, along with the identification of the spatial patterns of uniform, unimodal and bimodal flood seasons, provides a starting point to assess the existence of one dominant or multiple flood generating processes for distinct regions in Europe. For example, if the monthly flood seasonality distribution consists of a single peak change that ranges just over few months (similar to Cluster 5 and Cluster 6), then it is likely that the floods are generated by one temporally distinct driving process, such as snowmelt (see also above). However, if the temporal flood seasonality distribution is spread over several months it is likely that several drivers (rain, rain on snow, snowmelt or soil moisture) tend to cause floods. This seems to be the case is Cluster 4, which contains stations that are located at the eastern coast of the British Irish Isles and the northern Mediterranean coast, which have a different Köppen-Geiger climate classification.

20 Overall, the existence of a large-scale pattern of flood seasonality characteristics points to climate being the dominant large-scale control, with local catchment characteristics modulating the climatic inputs. Given the variety of flood generation processes across Europe and their distinct local interplay, the attribution of the detected large scale-pattern to specific climate characteristics and weather patterns is beyond the scope of this study and merits a follow-up study.

25 The assessment presented here summarises the temporal flood seasonality distributions and the spatial patterns over the period 1960-2010. The timing of floods within this period, however, varies and changes in the flood seasonality distribution have

been linked to a changing climate. For example, shifts changes in the timing of floods have been observed (e.g. Arheimer and Lindström, 2015; Blöschl et al., 2017; Wilson et al., 2010). For example, the timing of snowmelt generated floods has shifted towards earlier in the season as a result of earlier snowmelt due to rising temperatures. This shift is projected to continue for as long as snowmelt is relevant for flooding (e.g. Teutschbein et al. (2015) for Swedish catchments).

- 5 If snow processes become less important due to higher temperatures in the distant future, flood seasonality patterns in north eastern Europe might change completely if other flood generation processes may become dominant. In Europe, more research is needed to determine how the spatial and temporal clusters of flood seasonality might change in future, due to the complexity of the flood generation processes (precipitation occurrence and temperature, and soil moisture), their interactions, and also their interactions with the physical catchment properties (Stewart, 2009).
- 10 If raising temperatures in the future result in diminished snow accumulation during winter, the annual maximum flood caused by spring snowmelt might be replaced by an annual maximum flood caused by increased precipitation depending on the season in which the rainfall occurs. The effect of increasing temperatures leading to earlier floods could also be masked by a concurrent precipitation increase in the cold season, resulting in higher snow accumulation and delayed melt (Kay and Crooks, 2014), causing the floods to occur later.
- 15 Due to differences in the flood generation processes and how they are captured by hydrological models, future projections of flooding diverge. This is particularly the case for floods generated by high intensity precipitation, which is difficult to project into the future (Kundzewicz et al., 2017). Additionally, not only the amount of precipitation determines flood generation, but also the spatio-temporal distribution and the antecedent soil moisture conditions, which will also affect the flood seasonality projects.

20

6 Conclusion

This study identifies spatially distinct regions with characteristic patterns of temporal flood occurrence. A transition in the pattern of mean seasonality is apparent, from winter floods in western Europe to late spring and early summer floods in eastern Europe, onto which (depending on the region) late spring to summer floods are superimposed.

The temporal concentration of floods around the mean date of flood occurrence is highest in north and north-eastern Europe and on the western lower latitude coasts. This is also apparent in the low temporal spread of floods (on average less than two months) and the high occurrence of stations with a unimodal flood season in the clusters located in these regions.

The occurrence of a bimodal flood seasonality distribution over the year is only detected in a small number of stations.

- 30 Therefore, bimodality in the temporal distribution of AMF can be considered a local phenomenon occurring in spatially distinct locations in Europe. Nevertheless, in these regions the existence of a distinct secondary flood season is of practical importance for example for reservoir and flood risk management.

Overall, the results suggest that for most of stations, the geographical location (including elevation) and hence regional climate is the most important factor influencing the timing of annual maximum floods in Europe. Therefore, the study can be

considered a contribution towards advancing the understanding of geographical and climate sensitivity of annual maximum floods and their temporal characteristics across Europe. Due to the strong spatial consistency of the clusters obtained, the results will also be important for an improved understanding of flood generation mechanisms at the European scale and the insights on the flood seasonality characteristics gained in this study provide a benchmark for the assessment of European-wide hydrological model output.

Data Availability. The data analysed in this study is based on the database from the works of Hall et al. 2015 and Blöschl et al. 2017 with additional some updates.

10 *Competing Interests.* The authors declare that they have no conflict of interest.

Acknowledgements. The research was supported by the ERC Advanced Grant “FloodChange” Project No. 291152. All calculations and Figures were produced using R (R-Core-Team, 2016). The following packages used in the study are acknowledged: ‘classInt’, ‘cluster’, ‘fpc’, ‘maptools’, ‘plot3D’, ‘plotrix’, ‘plyr’, ‘raster’, ‘RColorBrewer’, ‘rgdal’, and ‘rworldmap’. The authors would like to acknowledge relevant discussions with Rui Perdigão and thank all data providers and
15 fellow researchers involved in the data preparation.

References

- Arheimer, B. and Lindström, G.: Climate impact on floods: changes in high flows in Sweden in the past and the future (1911–2100), *Hydrol. Earth Syst. Sc.*, 19(2), 771–784, doi:10.5194/hess-19-771-2015, 2015.
- 20 Barnett, T. P., Adam, J. C. and Lettenmaier, D. P.: Potential impacts of a warming climate on water availability in snow-dominated regions, *Nature*, 438(7066), 303–309, 2005.
- Bayliss, A. C. and Jones, R. C.: Peaks-over-threshold flood database: Summary statistics and seasonality. IH Report No. 121, Institute of Hydrology, Wallingford, UK., 1993.
- 25 Beurton, S. and Thieken, A. H.: Seasonality of floods in Germany, *Hydrol. Sci. J.*, 54(1), 62–76, doi:10.1623/hysj.54.1.62, 2009.
- Blöschl, G., Hall, J., Parajka, J., Perdigão, R. A. P., Merz, B., Arheimer, B., Aronica, G. T., Bilibashi, A., Bonacci, O., Borga, M., Čanjevac, I., Castellarin, A., Chirico, G. B., Claps, P., Fiala, K., Frolova, N., Gorbachova, L., Gül, A., Hannaford, J., Harrigan, S., Kireeva, M., Kiss, A., Kjeldsen, T. R., Kohnová, S., Koskela, J. J., Ledvinka, O., Macdonald, N., Mavrova-Guirguinova, M., Mediero, L., Merz, R., Molnar, P., Montanari, A., Murphy, C., Osuch, M., Ovcharuk, V., Radevski, I., Rogger, M., Salinas, J. L., Sauquet, E., Šraj, M., Szolgay, J., Viglione, A., Volpi, E., Wilson, D., Zaimi, K. and Živković, N.: Changing climate shifts timing of European floods, *Science*, 357(6351), 588–590, doi:10.1126/science.aan2506, 2017.
- 35 Cunderlik, J. M., Ouarda, T. B. and Bobée, B.: On the objective identification of flood seasons, *Water Resour. Res.*, 40, W01520, doi:10.1029/2003WR002295, 2004.
- Everitt, B. S., Landau, S., Leese, M. and Stahl, D.: *Cluster Analysis*, Wiley Online Library., 2011.
- 40

- Garner, G., Van Loon, A. F., Prudhomme, C. and Hannah, D. M.: Hydroclimatology of extreme river flows, *Freshwater Biology*, doi:10.1111/fwb.12667, 2015.
- 5 Hall, J., Arheimer, B., Aronica, G. T., Bilibashi, A., Bohávc, M., Bonacci, O., Borga, M., Burlando, P., Castellarin, A., Chirico, G. B., Claps, P., Fiala, K., Gaál, L., Gorbachova, L., Gül, A., Hannaford, J., Kiss, A., Kjeldsen, T., Kohnová, S., Koskela, J. J., Macdonald, N., Mavrova-Guirguinova, M., Ledvinka, O., Mediero, L., Merz, B., Merz, R., Molnar, P., Montanari, A., Osuch, M., Parajka, J., Perdigão, R. A. P., Radevski, I., Renard, B., Rogger, M., Salinas, J. L., Sauquet, E., Sraj, M., Szolgay, J., Viglione, A., Volpi, E., Wilson, D., Zaimi, K. and Blöschl, G.: A European Flood Database: facilitating comprehensive flood research beyond administrative boundaries, *Proc. Int. Assoc. Hydrol. Sci.*, 370, 89–95, doi:10.5194/piahs-370-89-2015, 2015.
- 10 Hall, J., Arheimer, B., Borga, M., Brázdil, R., Claps, P., Kiss, A., Kjeldsen, T., Kriauciuniene, J., Kundzewicz, Z., Lang, M., Llasat, M. C., Macdonald, N., McIntyre, N., Mediero, L., Merz, B., Merz, R., Molnar, P., Montanari, A., Neuhold, C., Parajka, J., Perdigão, R. A. P., Plavcová, L., Rogger, M., Salinas, J. L., Sauquet, E., Schär, C., Szolgay, J., Viglione, A. and Blöschl, G.: Understanding flood regime changes in Europe: a state of the art assessment, *Hydrol. Earth Syst. Sc.*, 18, 2735–2772, doi:doi:10.5194/hess-18-2735-2014, 2014.
- 15 Hartigan, J. A. and Wong, M. A.: Algorithm AS 136: A k-means clustering algorithm, *Journal of the Royal Statistical Society. Series C (Applied Statistics)*, 28(1), 100–108, doi:10.2307/2346830, 1979.
- 20 Jeneiová, K., Kohnová, S., Hall, J. and Parajka, J.: Variability of seasonal floods in the Upper Danube River basin, *J Hydrol. Hydromech.*, 64(4), 357–366, doi:10.1515/johh-2016-0037, 2016.
- Kay, A. and Crooks, S.: An investigation of the effect of transient climate change on snowmelt, flood frequency and timing in northern Britain, *Int. J. Climatol.*, 34(12), 3368–3381, doi:10.1002/joc.3913, 2014.
- 25 Klaus, S., Kreibich, H., Merz, B., Kuhlmann, B. and Schröter, K.: Large-scale, seasonal flood risk analysis for agricultural crops in Germany, *Environ. Earth Sci.*, 75(18), 1–13, doi:10.1007/s12665-016-6096-1, 2016.
- 30 Köplin, N., Schädler, B., Viviroli, D. and Weingartner, R.: Seasonality and magnitude of floods in Switzerland under future climate change, *Hydrol. Process.*, 28, 2567–2578, doi:10.1002/hyp.9757, 2014.
- Kundzewicz, Z., Krysanova, V., Dankers, R., Hirabayashi, Y., Kanae, S., Hattermann, F., Huang, S., Milly, P., Stoffel, M., Driessen, P., Matczak, P., Quevauviller, P. and Schellnhuber, H.-J.: Differences in flood hazard projections in Europe-their causes and consequences for decision making, *Hydrol. Sci. J.*, 62(1), 1–14, 2017.
- 35 Lecce, S.: Spatial variations in the timing of annual floods in the southeastern United States, *J. Hydrol.*, 235(3), 151–169, doi:10.1016/S0022-1694(00)00273-0, 2000.
- 40 Mardia, K. V.: *Statistics of directional data*, Academic Press Inc. London., 1972.
- Mardia, K. V. and Jupp, P. E.: Tests of Uniformity and Tests of Goodness-of-Fit, in *Directional Statistics*, pp. 93–118, John Wiley & Sons, Inc., 2008.
- 45 Mediero, L., Kjeldsen, T., Macdonald, N., Kohnová, S., Merz, B., Vorogushyn, S., Wilson, D., Albuquerque, T., Blöschl, G., Bogdanowicz, E., Castellarin, A., Hall, J., Kobold, M., Kriauciuniene, J., Lang, M., Madsen, H., Gül, G. O., Perdigão, R. A. P., Roald, L. A., Salinas, J. L., Toumazis, A. D., Veijalainen, N. and Þórarinnsson, Ó.: Identification of coherent flood regions across Europe by using the longest streamflow records, *J. Hydrol.*, 528, 341–360, doi:10.1016/j.jhydrol.2015.06.016, 2015.

- Parajka, J., Kohnová, S., Merz, R., Szolgay, J., Hlavcová, K. and Blöschl, G.: Comparative analysis of the seasonality of hydrological characteristics in Slovakia and Austria, *Hydrol. Sci. J.*, 54(3), 456–473, doi:10.1623/hysj.54.3.456, 2009.
- R-Core-Team: R - A Language and Environment for Statistical Computing, Vienna, Austria. [online] Available from: <https://www.R-project.org/>, 2016.
- Rousseeuw, P. J.: Silhouettes: A graphical aid to the interpretation and validation of cluster analysis, *Journal of computational and applied mathematics*, 20, 53–65, doi:10.1016/0377-0427(87)90125-7, 1987.
- 10 Ryberg, K. R., Akyüz, F. A., Wiche, G. J. and Lin, W.: Changes in seasonality and timing of peak streamflow in snow and semi-arid climates of the north-central United States, 1910-2012, *Hydrol. Process.*, 30, 1208–1218, doi:10.1002/hyp.10693, 2016.
- Steinley, D.: Local optima in K-means clustering: what you don't know may hurt you., *Psychol. Methods*, 8(3), 294–304, doi:10.1037/1082-989X.8.3.294, 2003.
- 15 Stewart, I. T.: Changes in snowpack and snowmelt runoff for key mountain regions, *Hydrol. Process.*, 23(1), 78–94, doi:10.1002/hyp.7128, 2009.
- 20 Teutschbein, C., Grabs, T., Karlsen, R. H., Laudon, H. and Bishop, K.: Hydrological response to changing climate conditions: Spatial streamflow variability in the boreal region, *Water Resour. Res.*, 51(12), 9425–9446, doi:10.1002/2015WR017337, 2015.
- Vesanto, J.: Importance of Individual Variables in the k-Means Algorithm, in *Advances in Knowledge Discovery and Data Mining: 5th Pacific-Asia Conference, PAKDD 2001 Hong Kong, China, April 16-18, 2001 Proceedings*, edited by Cheung, David and Williams, Graham J. and Li, Qing, pp. 513–518, Springer Berlin Heidelberg, Berlin, Heidelberg., 2001.
- Wilson, D., Hisdal, H. and Lawrence, D.: Has streamflow changed in the Nordic countries? – Recent trends and comparisons to hydrological projections, *J. Hydrol.*, 394(3–4), 334–346, 2010.
- 30 Ye, S., Li, H.-Y., Leung, L. R., Guo, J., Ran, Q., Demissie, Y. and Sivapalan, M.: Understanding flood seasonality and its temporal shifts within the contiguous United States, *J. Hydrometeorol.*, 18(7), 1997–2009, doi:10.1175/JHM-D-16-0207.1, 2017.

35

Supplement:

Data Sources of the database used in this study and their respective data holders

Data Source Country/Project	Data Holder/Source/Project information
Albania	National Hydro-Meteorological Service Albania, Institute of GeoSciences, Energy, Water and Environment (IGEWE)
Austria	Hydrographic Services of Austria (HZB), Austrian Federal Ministry of Agriculture, Forestry, Environment and Water Management
Bosnia and Herzegovina	Hydrological Yearbooks of the former Republic of Yugoslavia
Bulgaria	Hydrological Yearbooks of the Rivers in Bulgaria, National Institute of Meteorology and Hydrology
Croatia	Meteorological and Hydrological Service of Croatia (DHMZ)
Czechia	Czech Hydrometeorological Institute
Denmark	Freshwater Scientific Data Centre, Danish Centre for Environment and Energy (DCE)
Estonia	Estonian Environment Agency (KAUR)
EWA	European Water Archive (EWA)
Finland	Finnish Environment Institute, Open information/Hydrology/Discharge(SYKE)
France	HYDRO database, French Ministry of Ecology, Sustainable Development and Energy
Germany	Federal Waterways and Shipping Administration (WSV)
Germany, Bavaria	Bavarian Environment Agency (LfU)
Germany, Brandenburg	Brandenburg State Office of Environment, Health and Consumer Protection (LUGV)
Germany, Hesse	Hessian Agency for Nature Conservation, Environment and Geology (HLNUG)
Germany, Lower Saxony	Lower Saxony Water Management, Coastal Defence and Nature Conservation Agency (NLWKN)
Germany, Mecklenburg-Vorpommern	State Office of Environment, Nature Protection and Geology of Mecklenburg-Vorpommern (LUNG)
Germany, North Rhine-Westphalia	North Rhine-Westphalia State Agency for Nature, Environment and Consumer Protection (LANUV),
Germany, Rhineland-Palatinate	State Office for the Environment (LfU), Rhineland-Palatinate
Germany, Saarland	The Saarland State Office for Environmental and Labour Protection (LUA)
Germany, Saxony	Saxon State Agency for Environment, Agriculture and Geology (LfULG)
Germany, Saxony-Anhalt	State Agency for Flood Defence and Water Management of Saxony-Anhalt (LHW)
Germany, Schleswig-Holstein	Schleswig-Holstein Agency for Coastal Defence, National Park and Marine Conservation (ACNM-SH)
Germany, Thuringia	Thuringian State Institute for the Environment and Geology (TLUG)
GRDC	The Global Runoff Data Centre, Koblenz, Germany
Greece	Hydroscope- Ministry for the Environment, Energy and Climate Change - Special Secretariat for Water
Hungary	General Directorate of Water Management, Hungary
Hungary	Lower Tisza District Water Directorate
HYDRATE	HYDRATE Project data base: Hydrometeorological Data Resources and Technology for Effective Flash Flood Forecasting
Ireland	Irish Environmental Protection Agency (EPA)
Ireland	Office of Public Works (OPW)
Italy	Former National Hydrographic Service (SIMN)
Italy	The Italian National Institute for Environmental Protection and Research (ISPRA)
Italy	National Research Council (CNR)

Italy, Bolzano, South Tyrol Region	Hydrological Services, Autonomous Province of Bozen/Bolzano - South Tyrol
Italy, Emilia-Romagna Region	Regional Agency for the Environmental Protection (ARPA), Emilia-Romagna
Italy, Lazio & Umbria	Bencivenga M., Calenda G. and Mancini C.P., 2001.
Italy, Piedmont Region	Italian National Agency for Electricity (ENEL)
Italy, Piedmont Region	Research Institute for Hydro-Geologic Protection (IRPI)
Italy, Piedmont Region	Regional Agency for the Environmental Protection (ARPA), Piemonte
Italy, Po Region	Basin Authority of the Po River
Italy, Sicily Region	Water Observatory - Sicily Region
Italy, Trentino Region	Civil Protection Department, Autonomous Province of Trento
Italy, Tuscany Region	Regional Functional Centre of Meteo-Hydrological Monitoring, Tuscany
Italy, Veneto Region	Regional Agency for the Environmental Protection (ARPA), Veneto
Latvia	Latvian Environment, Geology and Meteorology Centre
Lithuania	Lithuanian Hydrometeorological Service under the Ministry of Environment
Netherlands	Dutch Ministry of Infrastructure and the Environment - Rijkswaterstaat
Norway	Database Hydra II; Norwegian Water Resources and Energy Directorate (NVE)
Poland	Institute of Meteorology and Water Management National Research Institute (IMGW-PIB)
Portugal	Portuguese Environmental Agency National Information System for Water Resources of Portugal (SNIRH)
Republic of Macedonia	National Hydrometeorological Service, Republic of Macedonia
Russia	Ministry of Natural Resources and Ecology of the Russian Federation
Russia	State Water Cadastre, State Hydrological Institute, Lomonosov Moscow State University
Russia	AIS GMVO, Russian Federal Agency for Water Resources
Serbia	Republic Hydrometeorological Service of Serbia (RHSS)
Slovakia	Slovak Hydrometeorological Institute, Bratislava (SHMI)
Slovenia	Slovenian Environment Agency (ARSO)
Spain	Centre for Hydrographic Studies of CEDEX, Ministry of Agriculture, Food and Environment, Spain
Sweden	Swedish Meteorological and Hydrological Institute (SMHI)
Switzerland	Federal Office for the Environment (BAFU)
Turkey	General Directorate of Electrical Power Resources Survey and Development Administration (EIE), Turkey
Ukraine	Hydrological Department, Ukrainian Hydrometeorological Institute (UHMI)
Ukraine	Hydrometeorological Institute, Odessa State Environmental University (OSENU)
United Kingdom	UK National River Flow Archive (NRFA)
